Evaluating Electrochemical Accessibility of $4f^n5d^1$ and $4f^{n+1}$ Ln(II) Ions in $(C_5H_4SiMe_3)_3Ln$ and $(C_5Me_4H)_3Ln$ Complexes

SCHOLARONE™
Manuscripts

Evaluating Electrochemical Accessibility of $4f^n5d^1$ and $4f^{n+1}$ Ln(II) Ions

in $(C_5H_4SiMe_3)_3Ln$ and $(C_5Me_4H)_3Ln$ Complexes

Michael T. Trinh, Justin C. Wedal, and William J. Evans*

Department of Chemistry, University of California, Irvine, California 92697-2025, United States

Email: wevans@uci.edu

ABSTRACT

The reduction potentials for a series of Cp'_3Ln complexes ($Cp' = C_5H_4SiMe_3$, Ln = lanthanide) were determined via electrochemistry in THF with $[^nBu_4N][BPh_4]$ as the supporting electrolyte. The Ln(III)/Ln(II) reduction potentials for Ln = Eu, Yb, Sm, and Tm ($-1.07 - -2.83$ V) follow the expected trend for stability of $4f^7$, $4f^{14}$, $4f^6$, and $4f^{13}$ Ln(II) ions, respectively. The reduction potentials for Ln = Pr, Nd, Gd, Tb, Dy, Ho, Er, and Lu, that form $4f^n5d^1$ Ln(II) ions (n = 0–14), fall in a narrow range of -2.95 V to -3.14 V. Only cathodic events were observed for La and Ce at -3.36 V and -3.43 V, respectively. The reduction potentials of the Ln(II) compounds $[K(2.2.2-cryptand)][Cp'_3Ln]$ (Ln = Pr, Sm, Eu) match those of the Cp'_3Ln complexes. The reduction potentials of nine $(C_5Me_4H)_3Ln$ complexes were also studied and found to be 0.05–0.24 V more negative than those of the Cp'_3Ln compounds.

INTRODUCTION

For many years, it was assumed that $4f^7$ Eu(II), $4f^{14}$ Yb(II), and $4f^6$ Sm(II) were the only +2 lanthanide ions accessible in solution.[1–3] The availability of these ions was attributed to the quantum mechanical stabilization and symmetric nature of the half-filled and filled-shells and the $4f^6$ configuration that approached a half-filled shell. Chemical[4–6] and electrochemical[7,8] studies were consistent with this idea, with Eu(II) being the most stable, followed by Yb(II) and then

Sm(II). Ln(III)/Ln(II) reduction potentials for the $4f^n \rightarrow 4f^{n+1}$ couples, estimated on the basis of thermochemical and electrochemical data (see SI for a compilation), suggested the Ln(II) ions of the other lanthanides were so negative that the Ln(II) ions would react with any solvent.[3,9,10] Tm(II), Dy(II), and Nd(II) were known in the solid state, but were not expected to exist in solution[2,11] until 1997-2001 when Bochkarev and co-workers showed that molecular species of $4f^{13}$ Tm(II), $4f^{10}$ Dy(II), and $4f^4$ Nd(II) could be synthesized.[4,12,13] The $4f^{13}$ Tm(II) ion was the next most likely Ln(II) species since it was approaching a filled shell, but the other two ions did not have electron configurations that could be rationalized by this method. Since no other Ln(II) ions were known even in the solid state, it was believed that Eu(II), Yb(II), Sm(II), Tm(II), Dy(II), and Nd(II) were the only lanthanides that could be isolable in the +2 oxidation state.

In 2008, Lappert reported La(II) and Ce(II) species via reduction of tris(cyclopentadienyl) complexes[14] and by 2013, Ln(II) were known for all the rest of the lanthanide series (excluding radioactive Pm) and yttrium using this reduction method (Scheme 1).[15–21] Lappert reported electrochemical measurements on Cp″₃La and a reversible couple was observed with an $E_{1/2}$ value
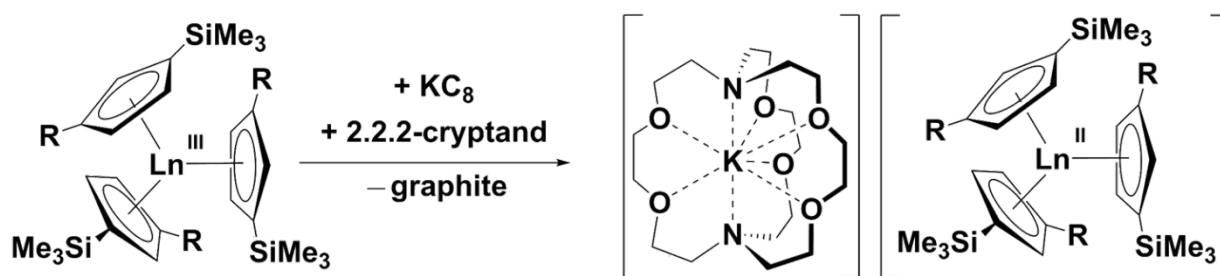
R = H; Ln = Y, La, Ce, Pr, Nd, Sm, Gd, Tb, Dy, Ho, Er, Tm, Lu
R = SiMe₃; Ln = La, Ce, Pr, Nd

Scheme 1. Reduction of $(C_5R_5)_3Ln$ to form Ln(II) complexes.

of -2.80 V vs Fc⁺/Fc.[22] However, electrochemical analysis of the other Ln(III)/Ln(II) reduction potentials has focused predominantly on the traditional six Ln(II) (Ln = Nd, Sm, Eu, Dy, Tm, and

Yb) ions with $4f^{n+1}$ electron configurations[12,13] despite the availability of every lanthanide metal in

the +2 oxidation state.

The absence of electrochemical measurements on the non-traditional Ln(III)/Ln(II) redox

couples is due in part to the high reactivity of the new $4f^n5d^1$ Ln(II) ions and the very negative

reduction potentials needed to form them. The most polar solvent that is inert to these Ln(II)

ions[23,24] is THF which leads to a large internal resistance and large peak separations.[25,26] In

addition, Ln(II) species often react with common supporting electrolytes. Recent electrochemical

studies of low oxidation state actinide complexes have shown that $[^nBuN_4][BPh_4]$ is suitable for

strongly reducing f element systems.[27–31]

We now find that $[^nBuN_4][BPh_4]$ is an excellent supporting electrolyte for lanthanide

systems. Here, we report the successful electrochemical determination of the Ln(III)/Ln(II)

reduction potential across the entire Cp'_3Ln ($Cp' = C_5H_4SiMe_3$) series using $[^nBu_4N][BPh_4]$ in

THF. Additionally, the electrochemistry of three Ln(II) complexes, $[K(crypt)][Cp'_3Ln]$ (crypt =

2.2.2-cryptand), is reported to verify the data obtained from Cp'_3Ln studies. Also reported are

reduction potentials of nine Cp^{tet}_3Ln ($Cp^{tet} = C_5Me_4H$) compounds that were analyzed to

investigate the impact of the electron-donation strength of the ligand on the reduction potentials of

the lanthanide complexes.

EXPERIMENTAL DETAILS

All manipulations and syntheses described below were conducted with the rigorous

exclusion of air and water using standard Schlenk line and glovebox techniques under an argon

atmosphere. Solvents were sparged with UHP argon and dried by passage through columns

containing Q-5 and molecular sieves prior to use. $Cp'_3Ln,$[15–18,32] $[K(crypt)][Cp'_3Ln],$[17,18] and

Cp^{tet}_3Ln[33–36] were synthesized according to literature procedures. $[^nBu_4N][BPh_4]$ (Sigma,

electrochemical grade >99%) was recrystallized from acetone three times and dried at 80 °C and

10^{-5} Torr overnight before use. $(C_5Me_5)_2Fe$ (Aldrich) was purified by sublimation before use.

Electrochemical measurements were collected with a freshly made THF solution of supporting

electrolyte with a glassy carbon working electrode, platinum wire counter electrode, and silver

wire pseudo-reference electrode with a Princeton Applied Research PARSTAT 2273 Advanced

Electrochemical System and referenced with internal standard $(C_5Me_5)_2Fe$. Internal resistance was

measured for each solution and resistance was manually compensated by approximately 90% of

the measured value. All scans on Cp'_3Ln and Cp^{tet}_3Ln were in the cathodic direction while scans

on $[K(crypt)][Cp'_3Ln]$ were in the anodic direction.

General Electrochemistry Procedure. Inside the glovebox, a stock 100 mM

$[^nBu_4N][BPh_4]$ electrolyte solution was freshly prepared in THF. Between 1–2 mL of this solution

were transferred to a 20 mL scintillation vial and a cyclic voltammogram of this solution was

collected to verify the electrolyte solution was free of impurities. Roughly 10-20 mg of the Ln

compound were dissolved in the same electrolyte solution to yield approximately a 10 mM

solution. Electrodes were placed into the vial and the vial was left open to the glovebox

atmosphere during data collection. The internal resistance was measured and cyclic voltammetry

experiments were then recorded. $(C_5Me_5)_2Fe$ was added to the solution following all data

collection, and a single scan was recorded to measure the internal standard redox event.

RESULTS

Electrochemical Protocol. Cyclic voltammetry experiments were performed using a

glassy carbon disc working electrode, a platinum wire counter electrode, and a silver wire pseudo-

reference electrode. Freshly-made 100 mM solutions of $[^nBu_4N][BPh_4]$ in THF provided the

supporting electrolyte. All potentials are reported versus the ferrocenium/ferrocene (Fc⁺/Fc)

couple, which is reported as −0.40 V vs NHE.[37] Decamethylferrocene, $(C_5Me_5)_2Fe$, which has a reduction potential of −0.495 V vs Fc^+/Fc under the present experimental conditions,[27] was used as an internal standard for all experiments.

$(C_5H_4SiMe_3)_3Ln.$ The Cp'_3Ln series was chosen for this study since Cp'_3Ln can be synthesized for the entire lanthanide series (excluding radioactive promethium), as well as for yttrium.[20] The reduction potentials measured for the Cp'_3Ln complexes are given in Table 1.

The cyclic voltammograms of all the Cp'_3Ln complexes, except for Cp'_3La and Cp'_3Ce, exhibit a quasi-reversible event assigned to the Ln(III)/Ln(II) redox couple (see SI).   A representative example of Cp'_3Tb is shown in Figure 1. The ΔE_{pp} varies from 0.18 V to 1.08 V, as was previously found for the actinide and lanthanide electrochemistry in THF using $[^nBu_4N][BPh_4]$ or $[^nBu_4N][OTf]$.[27,38]
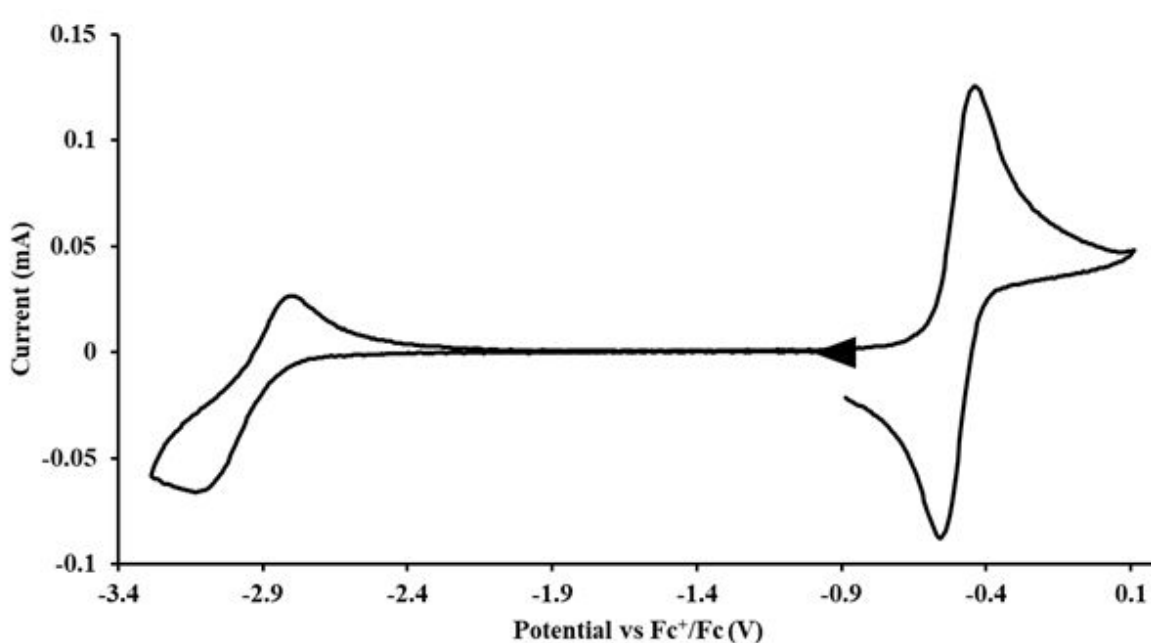

Figure 1. Cyclic voltammogram of Cp'_3Tb with the internal standard $(C_5Me_5)_2Fe$ at $v = 200$ mV/s. The event assigned to the Tb(III)/Tb(II) couple is centered at −2.95 V. The event at −0.495 V is due to the internal standard.

Variations in scan rate resulted in minimal change to the $E_{1/2}$ value, see SI. The cyclic voltammograms for Cp$'_3$La and Cp$'_3$Ce displayed only cathodic events (Figure 2). In both cases, the processes are irreversible up to scan rates of $v = 800$ mV / s.
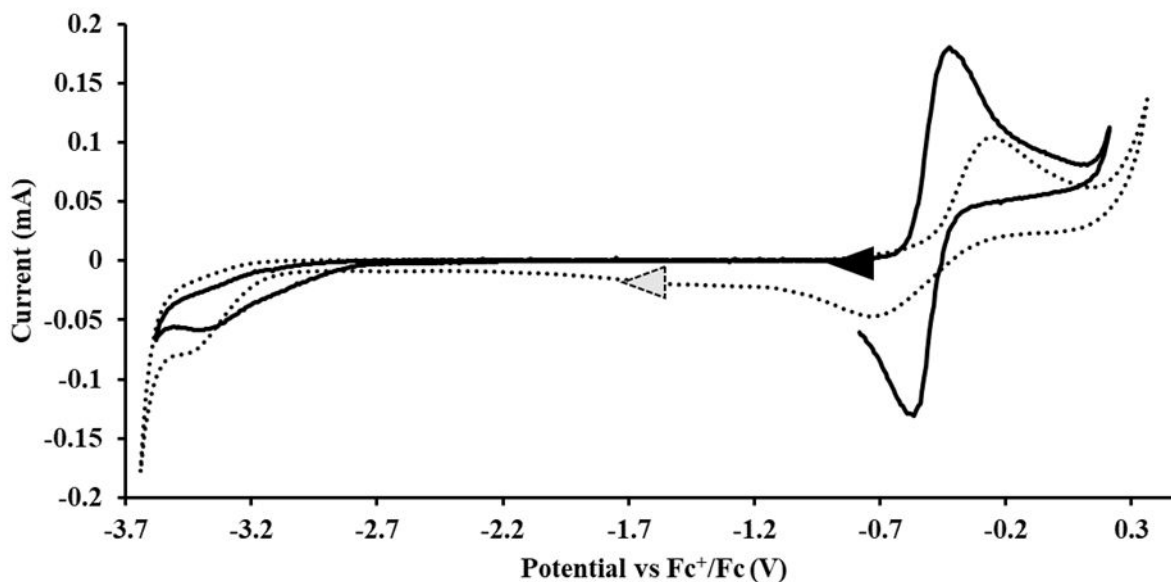

Figure 2. Cyclic voltammogram of Cp$'_3$La (solid) and Cp$'_3$Ce (dotted) with the internal standard (C$_5$Me$_5$)$_2$Fe at $v = 200$ mV/s. The events centered at -0.495 V are due to the internal standard.

(C$_5$Me$_4$H)$_3$Ln. The Cp$^{tet}_3$Ln compounds were also studied via electrochemistry to determine how the ligand electron-donating strength affects the Ln reduction potential. Ln(II) complexes with the Cp^{tet} ligand set, i.e. [K(crypt)][Cp$^{tet}_3$Ln], have been isolated only for the larger lanthanide metals Ln = La, Ce, Pr, Nd, Sm, Gd, Tb, and Dy. The redox couples observed in the cyclic voltammograms for Cp$^{tet}_3$Ln are summarized in Table 3 and Figure 4 shows a representative example for Cp$^{tet}_3$Gd. Interestingly, with this ligand set, both E_{PA} and E_{PC} events are observed for Cp$^{tet}_3$La and Cp$^{tet}_3$Ce, the latter of which has the most negative $E_{1/2}$. Overall, the reduction potentials for the Cp$^{tet}_3$Ln series are more negative than the Cp$'_3$Ln series which is consistent with the electron-donating strength of the ligand.[27,39–41]

Table 1. Ln(III)/Ln(II) reduction potentials of Cp′$_3$Ln with 100 mM [^{n}Bu$_4$N][BPh$_4$] supporting electrolyte in THF at $v = 200$ mV / s.

Ln	E_{PC} (V)	E_{PA} (V)	Ln(III)/Ln(II) $E_{1/2}$ (V)
Y	−3.12	−2.94	−3.06
La	−3.36	N/A[a]	N/A
Ce	−3.43	N/A[a]	N/A
Pr	−3.35	−2.93	−3.14
Nd	−3.33	−2.93	−3.14
Sm	−2.76	−2.06	−2.41
Eu	−1.61	−0.53	−1.07
Gd	−3.31	−2.64	−2.98
Tb	−3.10	−2.80	−2.95
Dy	−3.05	−2.86	−2.96
Ho	−3.12	−2.92	−3.02
Er	−3.14	−2.90	−3.02
Tm	−3.04	−2.63	−2.83
Yb	−2.02	−1.27	−1.64
Lu	−3.21	−3.03	−3.12

[a] Denotes the absence of a return oxidation in the cyclic voltammogram.

Table 2. Ln(III)/Ln(II) Reduction potentials for Cp′$_3$Ln and [K(crypt)][Cp′$_3$Ln] compounds with 100 mM [^{n}Bu$_4$N][BPh$_4$] supporting electrolyte in THF at $v = 200$ mV / s.

	E_{PC} (V)	E_{PA} (V)	Ln(III)/Ln(II) $E_{1/2}$ (V)
Cp′$_3$Pr	−3.35	−2.93	−3.14
[K(crypt)][Cp′$_3$Pr]	−3.36	−2.93	−3.15
Cp′$_3$Sm	−2.76	−2.06	−2.41
[K(crypt)][Cp′$_3$Sm]	−2.76	−2.06	−2.41
Cp′$_3$Eu	−1.61	−0.53	−1.07
[K(crypt)][Cp′$_3$Eu]	−1.48	−1.03	−1.26
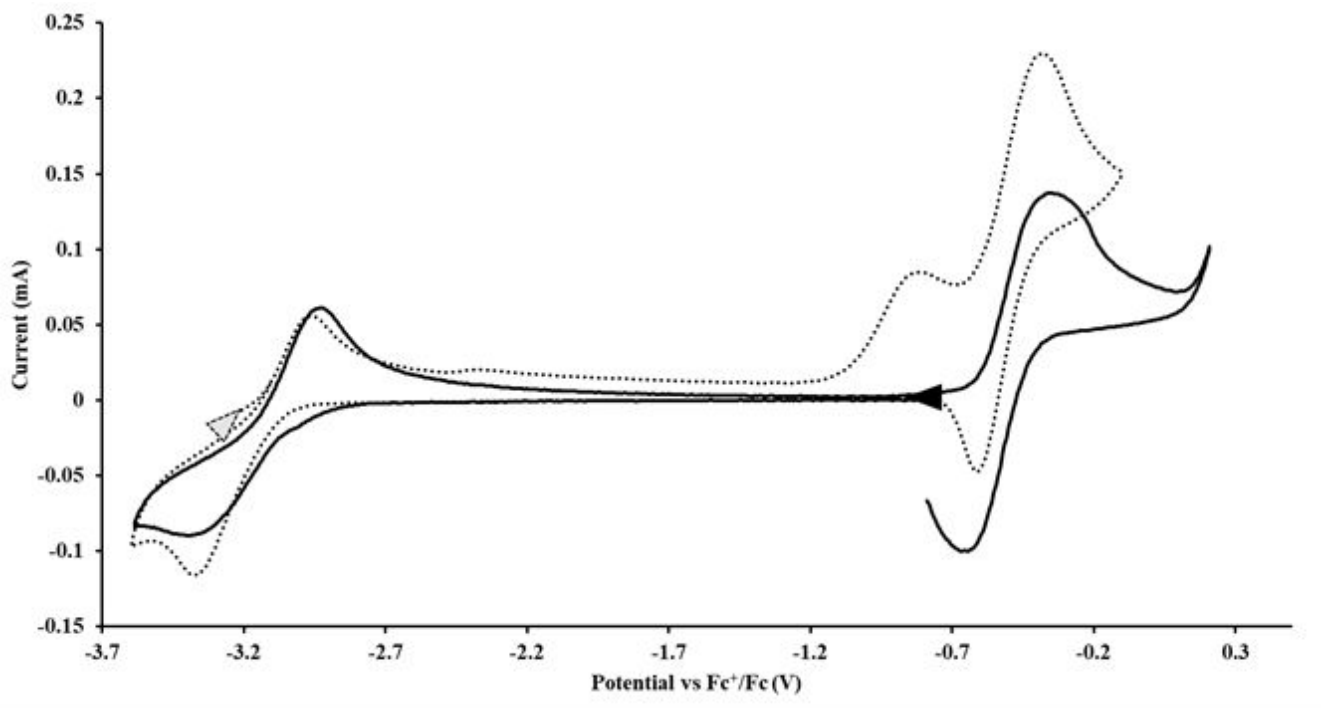
Figure 3. Cyclic voltammogram of Cp′$_3$Pr (solid) and [K(crypt)][Cp′$_3$Pr] (dashed) with the internal standard $(C_5Me_5)_2$Fe at $v = 200$ mV/s. The events centered at -3.14 V are assigned to the Pr(III)/Pr(II) couple, the anodic event at -0.35 V in the voltammogram of [K(crypt)][Cp′$_3$Pr] is likely a ligand-based event, and the event centered at -0.495 V is due to the internal standard.

Table 3. Ln(III)/Ln(II) reduction potentials of the Cp$^{tet}_3$Ln compounds with 100 mM [^{n}Bu$_4$N][BPh$_4$] supporting electrolyte in THF at $v = 200$ mV / s.

Ln	E_{PC} (V)	E_{PA} (V)	Ln(III)/Ln(II) $E_{1/2}$ (V)
La	−3.48	−3.22	−3.35
Ce	−3.32	−3.22	−3.37
Pr	−3.51	−3.22	−3.27
Nd	−3.27	−3.11	−3.19
Sm	−2.77	−2.43	−2.60
Gd	−3.12	−2.95	−3.04
Tb	−3.19	−3.04	−3.12
Dy	−3.29	−3.10	−3.20
Ho	−3.24	−3.11	−3.18
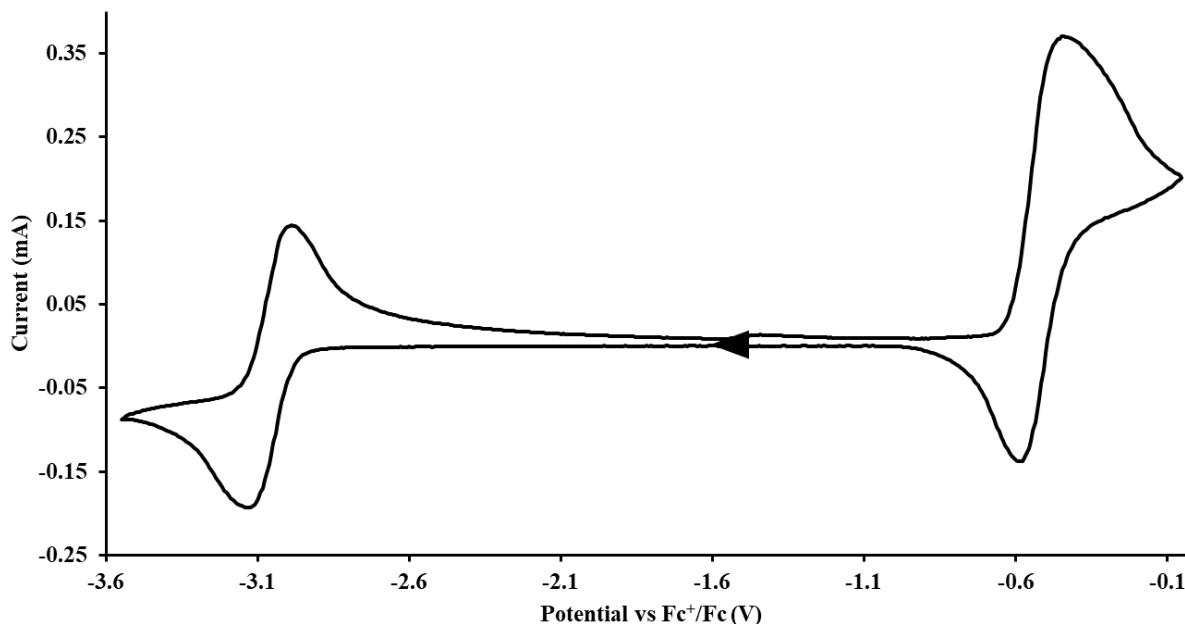
Figure 4. Cyclic voltammogram of Cp^{tet}_3Gd with the internal standard $(C_5Me_5)_2Fe$ at $v = 200$ mV/s. The event centered at -3.04 V is assigned to the Gd(III)/Gd(II) couple and the event centered at -0.495 V is due to the internal standard.

DISCUSSION

Using $[^nBu_4N][BPh_4]$ as a supporting electrolyte, it was possible for the first time to collect electrochemical data on all the metals in the lanthanide series (except the radioactive Pm). This is because the Cp'_3 ligand set is the first to support Ln(II) ions across the series in complexes stable enough for electrochemical analysis.

Except for Cp'_3La and Cp'_3Ce, quasi-reversible cyclic voltammograms were obtained and the assignment of the redox couple to a Ln(III)/Ln(II) process was confirmed by analyzing the Ln(II) complexes $[K(crypt)][Cp'_3Ln]$ for Ln = Pr, Eu, and Sm. For Cp'_3La and Cp'_3Ce, it is likely that the Ln(II) product participated in a chemical reaction that interfered with the corresponding oxidation in the redox couple.

The [^{n}Bu$_4$N][BPh$_4$] supporting electrolyte also led to successful electrochemical analysis of Cp^{tet}$_3$Ln complexes. Since Cp^{tet} is a more electron-donating ligand than Cp′,[27,39–41] more negative reduction potentials for Cp^{tet}$_3$Ln compared to their Cp′$_3$Ln analogs were observed with shifts of 0.05–0.24 V, depending on the metal. In addition, the electrochemistry of Cp^{tet}$_3$La was more reversible than that of Cp′$_3$La, even though these are some of the most negative potentials measured. Hence, the electrochemical results appear to be quite sensitive to the specific metal and ligand. A plot of the E_{PC} for Cp′$_3$Ln vs E_{PC} for Cp^{tet}$_3$Ln is shown in Figure 5 (see SI for plots of $E_{1/2}$). The low $R^2 = 0.62$ value shows the variability of the data with metal and ligand and the lack of a consistent correlation.
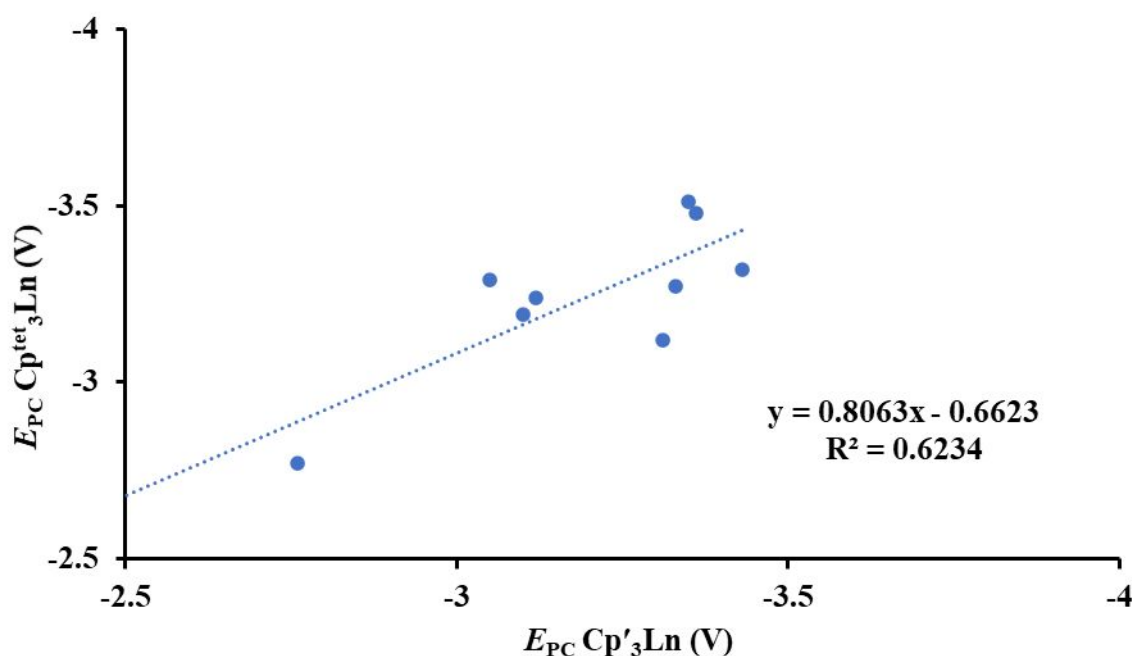

$$y = 0.8063x - 0.6623$$
$$R^2 = 0.6234$$

Figure 5. E_{PC} for Cp′$_3$Ln vs E_{PC} for Cp^{tet}$_3$Ln with "best fit" shown as the dotted line ($R^2 = 0.62$).

For the traditional 4f^{n+1} Ln(II) ions, the Ln(III)/Ln(II) reduction potentials of the Cp′$_3$Ln complexes follow the order of stability expected based on half-filled shells being more stable than filled shells. Hence, the couple for 4f^7 Eu(II) (−1.07 V) was less negative than that of 4f^{14} Yb(II) (−1.64 V). The Ln(II) ions with electron configurations approaching half-filled and filled subshells

are next, $4f^6$ Sm (II) (−2.41 V), and $4f^{13}$ Tm (−2.83 V). These data are valuable since they show

consistency with previous studies and match the known reactivity studies in the literature.

The reduction potentials of the non-traditional $4f^n5d^1$ Ln(II) ions were all more negative

than those of the traditional ions, a trend that is also consistent with chemical studies in the

literature. These $E_{1/2}$ values are plotted against the $4f^{n+1} \rightarrow 4f^n5d^1$ promotion energies for free

Ln(II) ions in the gas phase[42] (Figure 6). The metals (Ln = Eu, Yb, Sm, Tm) with the largest

promotion energy have the least negative reduction potentials and are metals that form $4f^{n+1}$ Ln(II)

ions. For all the other entries, the plot shows no correlation with the $4f^n + e^- \rightarrow 4f^n5d^1$ reduction

potential and the $4f^{n+1} \rightarrow 4f^n5d^1$ promotion energy. This lack of correlation and the narrow range

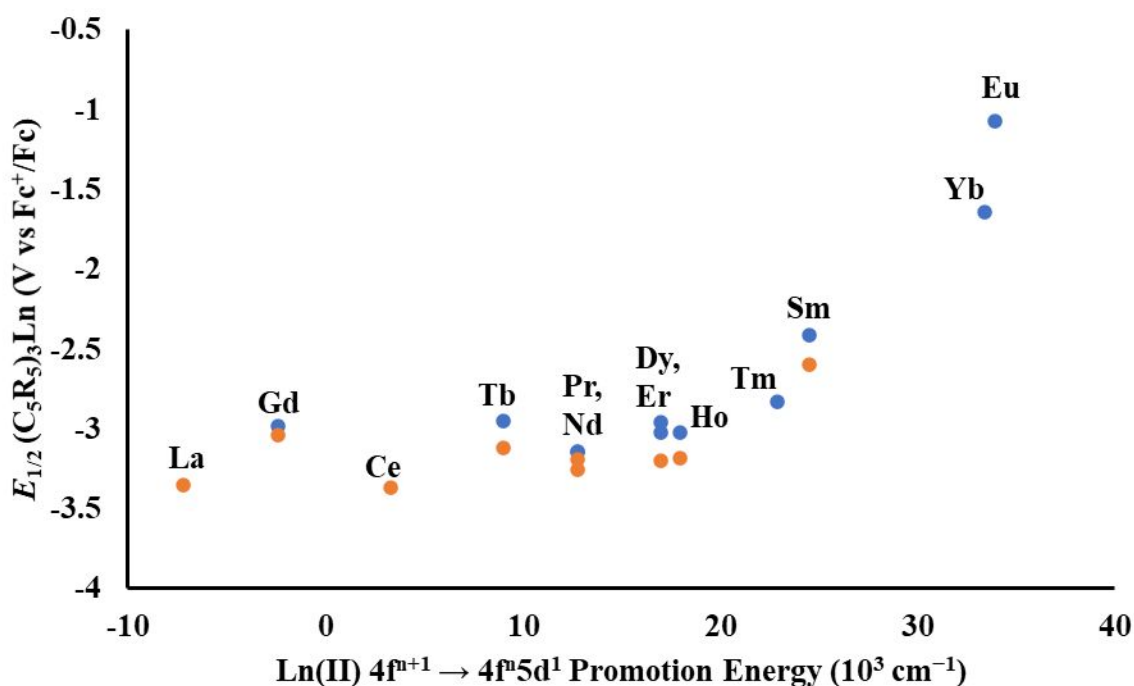

Figure 6. $E_{1/2}$ values of Cp′$_3$Ln (blue) and Cp$^{tet}_3$Ln (orange) versus $4f^{n+1} \rightarrow 4f^n5d^1$ promotion

energies for free Ln^{2+} ions in the gas phase.

11

of −2.95 V to −3.14 V reduction potentials for the other metals suggests that the electrochemical potential needed to add an electron to a $4f^n$ Ln(III) ion to make the $4f^n5d^1$ Ln(II) ion is similar for all these metals. There is also no obvious correlation between the reduction potentials and the number of 4f electrons in the $4f^n5d^1$ electron configuration (Table 4), but it does appear that the Ln(II) ions that have the most unpaired electrons in their electron configurations are the least difficult to reduce. Hence, $4f^75d^1$ Gd(II) with a half-filled 4f shell and $4f^85d^1$ Tb(II) with six formally unpaired 4f electrons have less negative reduction potentials compared to the other ions (Table 4). Since this analysis is at the single electron approximation level, this should only be noted as an observation that needs further evaluation in the future. It should also be noted that, at present, Gd, Dy, and Tb form more types of Ln(II) complexes with various ligands than the other metals.[18,23,33,43,44]

Table 4. $E_{1/2}$ and E_{PC} values for Cp′$_3$Ln in order of increasing reduction potential

Ln	$E_{1/2}$ (V)	E_{PC} (V)	n in $4f^n5d^1$	Number of unpaired f electrons
Tb	−2.95	−3.10	8	6
Dy	−2.96	−3.05	9	5
Gd	−2.98	−3.31	7	7
Ho	−3.02	−3.12	10	4
Er	−3.02	−3.14	11	4
Lu	−3.12	−3.21	14	0
Nd	−3.14	−3.33	3	3
Pr	−3.14	−3.35	2	2
La		−3.43	0	0
Ce		−3.36	1	1

The reduction potentials of Cp′$_3$Dy and Cp$^{tet}_3$Dy are of special interest since Dy(II) is a configurational crossover ion[17,20] that has a $4f^95d^1$ electron configuration in [K(crypt)][Cp′$_3$Dy][17] and a $4f^{10}$ configuration in [K(crypt)][Cp$^{tet}_3$Dy].[33] The more negative −3.20 V $E_{1/2}$ for Cp$^{tet}_3$Dy compared to −2.96 V for Cp′$_3$Dy is consistent with the large electron-donating power of Cp^{tet}. However, this means that it is easier to populate a 5d orbital in Cp′$_3$Dy than to add an electron to

the 4f valence orbitals of Cp^{tet}_3Dy. Again, this shows the strong dependence of the reduction potentials on ligands.

CONCLUSION

The reduction potentials for all the metals in the lanthanides series except Pm were determined in Cp'_3Ln complexes by electrochemical methods using $[^nBu_4N][BPh_4]$ as a supporting electrolyte in THF. Reactions involving $4f^n \rightarrow 4f^{n+1}$ reductions have the least negative $E_{1/2}$ values, -1.07 V to -2.83 V, and follow patterns for the stability of half-filled and filled-shell electron configurations. Reactions involving $4f^n$ to $4f^n5d^1$ reductions have more negative potentials that fall in the narrower range of -2.95 V to -3.14 V and the correlation with electron configuration is less clear. Cp^{tet}_3Ln complexes are more difficult to reduce which is consistent with the stronger electron-donating character of Cp^{tet} vs Cp', but there are variations on the Cp^{tet} vs Cp' data that are dependent on the specific metal.

AUTHOR INFORMATION

Corresponding Author

William J. Evans − Department of Chemistry, University of California, Irvine, California 92697 orcid.org/0000-0002-0651-418X; Email: wevans@uci.edu

Author

Michael T. Trinh − Department of Chemistry, University of California, Irvine, California 92697. orcid.org/0000-0001-6110-3546

Justin C. Wedal − Department of Chemistry, University of California, Irvine, California 92697. orcid.org/0000-0003-0437-8601

Notes

The authors declare no competing financial interest.

ACKNOWLEDGMENTS

REFERENCES

1   F. Nief, *Handbook on the Physics and Chemistry of Rare Earths*, Elsevier Science, Amsterdam, 2010.

2   G. Meyer, *Chem. Rev.*, 1988, **88**, 93–107.

3   L. R. Morss, *Chem. Rev.*, 1976, **76**, 827–841.

4   M. N. Bochkarev, *Coord. Chem. Rev.*, 2004, **248**, 835–851.

5   W. J. Evans, *Coord. Chem. Rev.*, 2000, **206–207**, 263–283.

6   G. A. Molander, *Chem. Rev.*, 1992, **92**, 29–68.

7   N. B. Mikheev, *Inorg. Chim. Acta*, 1984, **94**, 241–248.

8   A. M. Bond, G. B. Deacon and R. H. Newnham, *Organometallics*, 1986, **5**, 2312–2316.

9   S. G. Bratsch and J. J. Lagowski, *J. Phys. Chem.*, 1985, **89**, 3317–3319.

10   L. J. Nugent, R. D. Baybarz, J. L. Burnett and J. L. Ryan, *J. Phys. Chem.*, 1973, **77**, 1528–1539.

11   G. Meyer, in *The Rare Earth Elements: Fundamentals and Applications*, ed. D. A. Atwood, Wiley, New York, 2012, pp. 241–300.

12   M. N. Bochkarev, I. L. Fedushkin, A. A. Fagin, T. V. Petrovskaya, J. W. Ziller, R. N. R. Broomhall-Dillard and W. J. Evans, *Angew. Chem. Int. Ed.*, 1997, **36**, 133–135.

13   M. N. Bochkarev and A. A. Fagin, *Chem. Eur. J.*, 1999, **5**, 2990–2992.

14   P. B. Hitchcock, M. F. Lappert, L. Maron and A. V. Protchenko, *Angew. Chem. Int. Ed.*, 2008, **47**, 1488–1491.

15   M. R. MacDonald, J. W. Ziller and W. J. Evans, *J. Am. Chem. Soc.*, 2011, **133**, 15914–15917.

16   M. R. MacDonald, J. E. Bates, M. E. Fieser, J. W. Ziller, F. Furche and W. J. Evans, *J. Am. Chem. Soc.*, 2012, **134**, 8420–8423.

17   M. E. Fieser, M. R. MacDonald, B. T. Krull, J. E. Bates, J. W. Ziller, F. Furche and W. J. Evans, *J. Am. Chem. Soc.*, 2015, **137**, 369–382.

18   M. R. MacDonald, J. E. Bates, J. W. Ziller, F. Furche and W. J. Evans, *J. Am. Chem. Soc.*, 2013, **135**, 9857–9868.

19   C. T. Palumbo, L. E. Darago, C. J. Windor, J. W. Ziller and W. J. Evans, *Organometallics*, 2018, **37**, 900–905.

20   W. J. Evans, *Organometallics*, 2016, **35**, 3088–3100.

21   D. H. Woen and W. J. Evans, in *Handbook on the Physics and Chemistry of Rare Earths*, Elsevier B.V., 1st edn., 2016, pp. 1–57.

22   M. C. Cassani, M. F. Lappert and F. Laschi, *Chem. Commun.*, 1997, **2**, 1563–1564.

23   D. N. Huh, J. W. Ziller and W. J. Evans, *Dalton Trans.*, 2018, **47**, 17285–17290.

24   D. H. Woen, D. N. Huh, J. W. Ziller and W. J. Evans, *Organometallics*, 2018, **37**, 3055–3063.

25   I. Noviandri, K. N. Brown, D. S. Fleming, P. T. Gulyas, P. A. Lay, A. F. Masters and L. Phillips, *J. Phys. Chem. B*, 1999, **103**, 6713–6722.

26   K. J. Rountree, B. D. Mccarthy, E. S. Rountree, T. T. Eisenhart and J. L. Dempsey, *J. Chem. Educ.*, 2018, **95**, 197–206.

27   J. C. Wedal, J. M. Barlow, J. W. Ziller, J. Y. Yang and W. J. Evans, *Chem. Sci.*, 2021, **12**, 8501–8511.

28   C. J. Inman and F. G. N. Cloke, *Dalton Trans.*, 2019, **48**, 10782–10784.

29   D. E. Morris, R. E. Da Re, K. C. Jantunen, I. Castro-Rodriguez and J. L. Kiplinger, *Organometallics*, 2004, **23**, 5142–5153.

30   J. A. Hlina, J. R. Pankhurst, N. Kaltsoyannis and P. L. Arnold, *J. Am. Chem. Soc.*, 2016, **138**, 3333–3345.

31   J. C. Wedal, S. Bekoe, J. W. Ziller, F. Furche and W. J. Evans, *Dalton Trans.*, 2019, **48**, 16633–16640.

32   J. K. Peterson, M. R. MacDonald, J. W. Ziller and W. J. Evans, *Organometallics*, 2013, **32**, 2625–2631.

33   T. F. Jenkins, D. H. Woen, L. N. Mohanam, J. W. Ziller, F. Furche and W. J. Evans, *Organometallics*, 2018, **37**, 3863–3873.

34   C. J. Windorff, M. T. Dumas, J. W. Ziller, A. J. Gaunt, S. A. Kozimor and W. J. Evans, *Inorg. Chem.*, 2017, **56**, 11981–11989.

35   H. Schumann, M. Glanz, H. Hemling and F. Ekkehard Hahn, *Z. Anorg. Allg. Chem.*, 1995, **621**, 341–345.

36   W. J. Evans, D. B. Rego and J. W. Ziller, *Inorg. Chem.*, 2006, **45**, 10790–10798.

37   N. G. Connelly and W. E. Geiger, *Chem. Rev.*, 1996, **96**, 877–910.

38   D. N. Huh, S. R. Ciccone, S. Bekoe, S. Roy, J. W. Ziller, F. Furche and W. J. Evans, *Angew. Chem. Int. Ed.*, 2020, **59**, 2–8.

39   S. A. Moehring and W. J. Evans, *Organometallics*, 2020, **39**, 1187–1194.

40   S. A. Moehring and W. J. Evans, *Chem. Eur. J.*, 2020, **26**, 1530–1534.

41   C. E. Zachmanoglou, A. Docrat, B. M. Bridgewater, G. Parkin, C. G. Brandow, J. E. Bercaw, C. N. Jardine, M. Lyall, J. C. Green and J. B. Keister, *J. Am. Chem. Soc.*, 2002,

124, 9525–9546.

42   W. C. Martin, R. Zalubas and L. Hagan, *Atomic Energy Levels-The Rare-Earth Elements*,

U.S. Government Printing Office, Washington D.C., 1978.

43   A. J. Ryan, L. E. Darago, S. G. Balasubramani, G. P. Chen, J. W. Ziller, F. Furche, J. R.

Long and W. J. Evans, *Chem. Eur. J.*, 2018, **24**, 7702–7709.

44   M. E. Fieser, C. T. Palumbo, H. S. La Pierre, D. P. Halter, V. K. Voora, J. W. Ziller, F.

Furche, K. Meyer and W. J. Evans, *Chem. Sci.*, 2017, **8**, 7424–7433.

TOC Graphic:
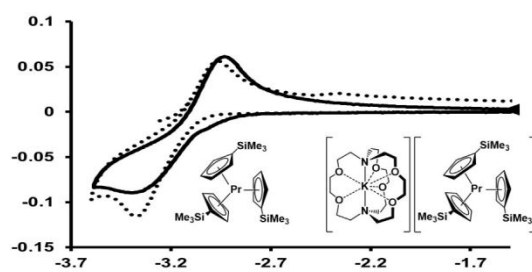
Electrochemical characterization of the Ln(III)/Ln(II) reduction potentials for the entire

lanthanide series and yttrium is reported for the $(C_5H_4SiMe_3)_3Ln$ complexes.